THE ASTROPHYSICAL JOURNAL, 459:298–306, 1996 March 1

THE EVOLUTIONARY PROPERTIES AND PECULIAR THERMAL PULSES OF METAL-DEFICIENT LOW-MASS STARS

SANTI CASSISI[1,2]
Osservatorio Astronomico di Collurania, via M. Maggini, I-64100 Teramo, Italy; cassisi@astrte.te.astro.it
VITTORIO CASTELLANI[3]
Università di Pisa, Dipartimento di Fisica, Piazza Torricelli 2, I-56100 Pisa, Italy;[3] vittorio@astr1pi.difi.unipi.it
AND
AMEDEO TORNAMBÈ[1]
Osservatorio Astronomico di Roma, I-00040 Monte Porzio, Italy; tornambe@coma.mporzio.astro.it
Received 1995 June 5; accepted 1995 August 31

ABSTRACT

We investigate the evolutionary behavior of low-mass star models with very low original metal content (log $Z = -10, -6, -5$) and $Y = 0.23$. The computations have been extended from the main sequence up to the double shell burning phase. Theoretical isochrones on the H-R diagram are presented for a range of ages spanning 7–15 $\times$ 10^9 yr. Attention has been paid to understand whether, and to what extent, stellar populations in the quoted metallicity range can produce currently observable RR Lyrae variables, the result being that, apart from an intrinsic scarcity of existing stars with such a composition, evolutionary properties are such that a vanishingly small number of RR Lyrae variables is expected to exist. However, if existing, metal-deficient RR Lyrae stars would present pulsational properties not easily distinguishable from those of standard Population II variables. Double shell burning structures are presented with discussion of the dependence of selected evolutionary features on the original metal content and, in particular, the occurrence of unusually strong He shell flashes following the first reignition of He shell burning. The H shell burning along the He intershell accretion phase and the following He shell burning reignition of the $M = 0.8\ M_\odot$, log $Z = -10$ model are discussed in detail. It is found that, even at the first episode of He shell reignition, the burning grows in so strong a flash that a convective shell develops at once, becoming large enough to interact with the H shell, so that a large amount of fresh protons is suddenly injected into the high-temperature He-burning region. After the third episode of hydrogen ingestion, it has not been possible to follow in detail the development of the instability since a time-dependent treatment of the convection would be required. It is however estimated that during the flash a maximum luminosity of $L_{\rm He} = 2.5 \times 10^8\ L_\odot$ would have been attained by He burning alone, in contrast with a maximum of $L_{\rm He} = 7.5 \times 10^4\ L_\odot$ attained at the first pulse of an equivalent structure with a normal metallicity. Whatever the further evolution of such an episode (a partial or total envelope ejection not being excluded), it remains the fact that a large amount of hydrogen is burned out at a very high temperature and in a very short time. Such an He shell flash could be regarded as the low-energy (intrisically nonexplosive) counterpart of the He detonation occurring in a more massive, more degenerate He shell, which induces a sub-Chandrasekhar explosion of the underlying white dwarf, suggesting that, in this last occurrence too, the hydrogen possibly surrounding the He layer could be similarly burned out at the moment of the He ignition. Thus, the present results may help to understand the lack of the hydrogen signature in the spectra of Type Ia supernovae, if such supernovae are mainly produced by sub-Chandrasekhar He detonations.

Subject headings: stars: abundances — stars: evolution — stars: interiors — stars: low-mass, brown dwarfs — stars: variables: other (RR Lyrae)

1. INTRODUCTION

The evolutionary properties of very metal poor stars have been addressed in a previous paper (Cassisi & Castellani 1993, Paper I), where the results of theoretical computations concerning the evolution of stars with log $Z = -10, -6$, and -4 were presented. In that paper, the computations extended from the main sequence up to the ignition of the He flash in low-mass structures, or well beyond the exhaustion of central helium in larger masses. The quoted investigation was mainly devoted to inferring information about the main contributors to the light from metal-deficient populations, as well as to investigation of the dependence on metallicity of the upper mass limit for the occurrence of carbon-degenerate cores ($M^{\rm up}$), below which, in absence of mass loss, intermediate-mass stars would end their lives with an explosive degenerate-carbon ignition.

The increasing observational evidence for metal-deficient stars populating our Galactic halo (Molaro & Bonifacio 1990; Molaro & Castelli 1990; Norris, Peterson, & Beers 1993; Primas, Molaro, & Castelli 1994; Sneden et al. 1994) and the suspected occurrence of metal-deficient stars in at least some nearby dwarf spheroidal galaxies, are now raising a renewed interest in the topic. However, we still lack a detailed theoretical knowledge of the expected dis-

[1] Università dell'Aquila, Dipartimento di Fisica, via Vetoio, I-67010 L'Aquila, Italy.
[2] Also, Observatoire de Paris-Meudon, Place Janssen, F-92195 Meudon, France.
[3] Osservatorio Astronomico di Collurania, via M. Maggini, I-64100 Teramo, Italy.

tribution of these stars in the C-M diagram, as needed to discuss on firm ground possible observational evidence. For instance, we still lack clear indications about the occurrence of RR Lyrae stars in metal-deficient populations, thus ignoring to what extent we can use the metallicity of these stars to map the metallicity of the Galactic halo.

According to such evidence, in this paper we extend previous computations of H-burning phases in low-mass stars, as given in Paper I for stars with log $Z = -10$ and -6, to the case log $Z = -5$, in order to fill the gap between log $Z = -6$ structures and the well-studied $Z = 10^{-4}$ evolutionary scenario (Castellani, Chieffi, & Pulone 1991; Bono et al. 1995). The investigation has been further implemented with theoretical evaluations of the He-burning phases, in order to gain information on the evolutionary behavior of these stars all along their nuclear-burning life, thus allowing us to put theoretical constraints on the occurrence of RR Lyrae pulsators among metal-deficient populations and on their properties.

All the evolutionary tracks were obtained by means of the FRANEC code (see, e.g., Castellani, Chieffi, & Straniero 1992 and references therein), using the same input physics as in Paper I, and adopting canonical semiconvection for the treatment of mixing during the central He-burning phase.

The present set of computations, added to those previously published, provides an extended and complete theoretical instrument to constrain observational data of very low metallicity stars and stellar systems.

Section 2 is devoted to presentation of the results of the evolutionary investigation, discussing theoretical isochrones in terms of cluster metallicity and/or age and, in particular, the expected H-R diagram location of horizontal-branch (HB) stars in connection with the aforementioned problem concerning the occurrence of RR Lyrae pulsators. Section 3 deals with the evolution of stellar structures in their advanced evolutionary phases and discusses some unexpected features of metal-deficient stars in the double shell burning phase. A final discussion and conclusions close the paper.

2. H- AND CENTRAL He-BURNING PHASES IN METAL-DEFICIENT LOW-MASS STARS

2.1. H-*Burning Phase*

As a first step, a set of evolutionary computations has been produced, which covers the H-burning phase of low-mass stars in the metallicity region previously mentioned for assumed values of the stellar masses in the range suitable for the purposes stated in § 1 (i.e., low-mass stars).

Table 1 presents some main physical quantities of the evolved models. For each value of the logarithm of the initial metal content, the first two columns give the mass of the evolved models and the logarithm of the luminosity in solar units at the red giant (RG) tip. The following three columns give the He core mass at the flash ($M_{cHe\text{-}F}$), the amount of extra helium brought to the surface by the first dredge-up (ΔY, by mass fraction), and the time elapsed before reaching the He flash ($\tau_{He\text{-}F}$), parameters to be used to constrain the evolutionary structures on their location on the zero-age horizontal branch (ZAHB).

Details of the evolutionary behavior during H-burning phases resemble closely those already discussed in Paper I. Therefore, the discussion will not be repeated here. Figure 1 shows selected isochrones for H-burning stars for the

TABLE 1

PHYSICAL QUANTITIES OF EVOLVED MODELS

M ($M_\odot$)	log ($L_{tip}/L_\odot$)	$M_{cHe\text{-}F}$ ($M_\odot$)	ΔY	$\tau_{He\text{-}F}$ (10^9 yr)
		log $Z = -10$		
0.7.....	2.382	0.507	0.000	24.907
0.8.....	2.376	0.506	0.000	15.417
1.0.....	2.340	0.491	0.000	7.063
1.1.....	1.800	0.375	0.000	5.066
		log $Z = -6$		
0.7.....	3.065	0.531	0.000	24.831
0.8.....	3.055	0.529	0.002	15.346
1.0.....	3.006	0.519	0.008	7.014
1.1.....	2.922	0.504	0.011	5.059
		log $Z = -5$		
0.7.....	3.171	0.520	0.001	24.831
0.8.....	3.156	0.516	0.004	15.241
1.0.....	3.122	0.509	0.012	6.966
1.1.....	3.083	0.501	0.015	5.035

various selected metallicities and for the labeled age intervals. Note that for the case log $Z = -10$ the lower limiting age has been fixed at 7×10^9 yr since for still lower ages one is dealing with stars of $\sim 1.2\ M_\odot$ or more, which fail to become red giants and will ignite helium near their main-sequence locations (see Paper I).

As expected, it is found that, for any given age, a decrease of the metallicity from log $Z = -5$ to log $Z = -6$ makes the turnoff location hotter and brighter, whereas the tip of the RG branch becomes fainter. However, Figure 1 shows that a further decrease of the metallicity down to log $Z = -10$ has only a minor effect on the location of the turnoff, whereas the RG tip becomes even fainter. According to the discussion given in Paper I, this has to be taken as

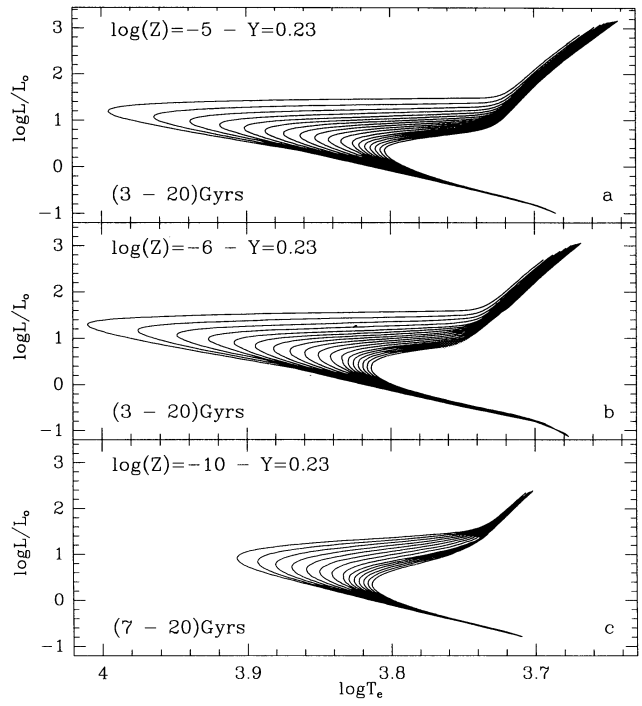

FIG. 1.—Cluster isochrones for H-burning phases for the labeled range of ages with 1 Gyr intervals and for the given cluster metallicity.

evidence that the turnoff location is governed by the vanishing influence of the opacity of heavy elements, whereas the energy production during the central H-burning phase is dominated by *p-p* burning, thus remaining unaffected by variations in the abundance of CNO elements. Conversely, one finds that CNO burning and, thus, the abundance of CNO nuclei continues to play a major role during the H shell burning phase, thus governing the luminosity of the RG tip down to $\log Z = -10$.

2.2. *Central* He *Burning*

To approach the problem of the evolutionary behavior of the He-burning phases, it is necessary to make some assumptions on the age of the stellar population, that is, on the original mass of the evolving giants, a value that represents an obvious upper limit for the mass of the He-burning models. In order to cover a reasonable range of ages, we assumed for the quoted original mass the values 0.8 and 1.0 $M_\odot$. Data in Table 1 show that this choice corresponds to cluster ages on the order of 15×10^9 and 7×10^9 yr, respectively. From Table 1, it is also possible to infer that such age variation implies a small, but not negligible, variation in the mass size of the He core at He flash ($M_{cHe\text{-}F}$). This difference has been taken into account in producing, for each age, ZAHB structures.

Figure 2 shows the paths in the H-R diagram of the computed set of HB models. Models derived from 0.8 $M_\odot$ progenitors are shown in the left panels while the right panels refer to models having as progenitors the 1.0 $M_\odot$ star model. The models cover a range of masses from 0.55 $M_\odot$ up to a maximum mass of 0.8 or 1.0 $M_\odot$, respectively, with steps in mass of 0.05 $M_\odot$. Included in the set are some additional hot models whose mass values are labeled in the figure. Dashed lines in Figure 2 mark the boundaries of the RR Lyrae instability strip, approximately taken at $\log T_e = 3.8$–3.9 (see, e.g., Sandage 1990). Open squares in the right panels show the ZAHB location of models with the same mass, but from a 0.8 $M_\odot$ progenitor.

An analysis of Figure 2 shows that the different assumptions about the mass of the progenitor (i.e., on the cluster age) is obviously reflected in the larger masses allowed to populate the red side of the HB of younger clusters. Models with the same mass but different progenitors show only small differences in H-R diagram location. The evidence that the variation increases when dealing with lower metallicities and/or hotter stellar models is the expected result of the increasing variations of $M_{cHe\text{-}F}$ and of the relative variations of the residual H-rich envelope surrounding hot, low-mass HB stars. As an evidence for the envelope-dominated evolution of hot stars, let us notice that in Figure 2 the two

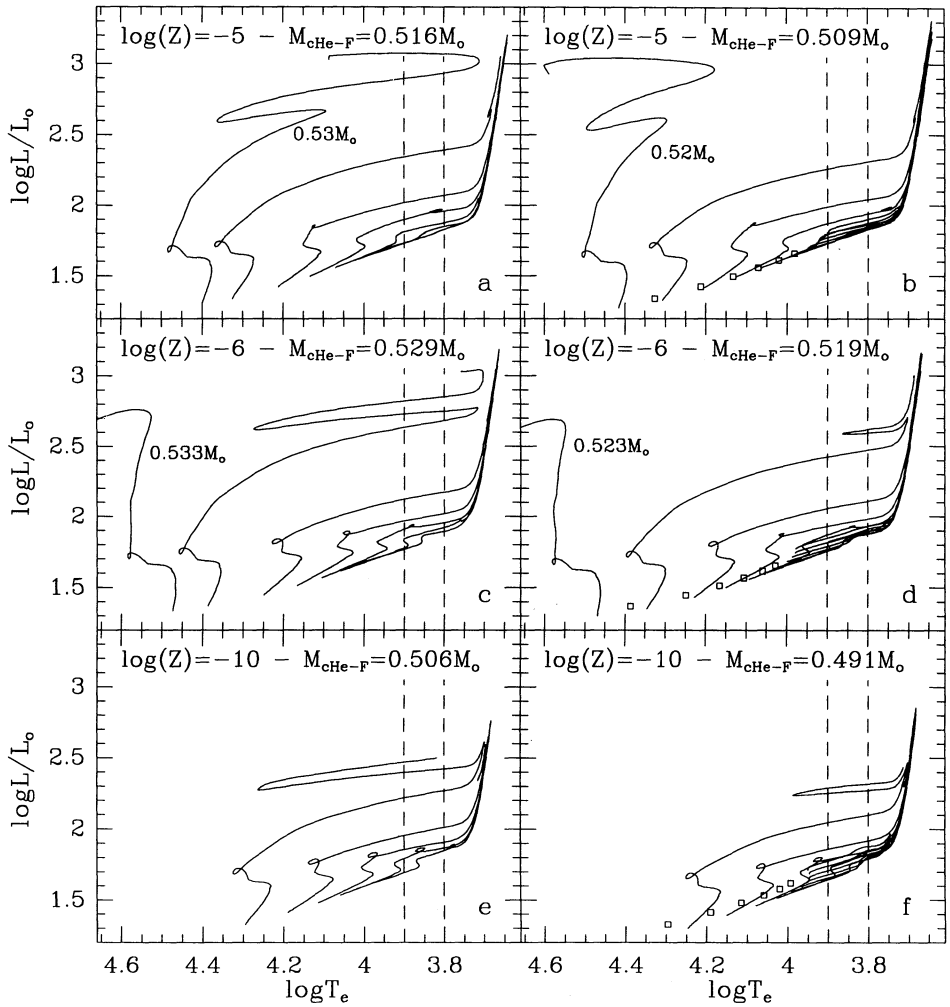

FIG. 2.—Evolutionary path in the H-R diagram of selected He-burning models, assuming an initial mass for the progenitor of 0.8 $M_\odot$ (*left*) and 1.0 $M_\odot$ (*right*) and various amount of mass loss (see § 2.2). The adopted chemical composition is labeled in each plot. In the right panels, squares show the location of ZAHB models with the same mass from the left panels. Dashed lines show the approximate boundaries of the RR Lyrae instability strip.

extreme models with log $Z = -5$ failing to reach the asymptotic giant branch (AGB) have envelopes of 0.011 and 0.014 $M_\odot$. Model with more massive envelopes experience a closer approach to the AGB, as expected on theoretical grounds (Dorman, Rood, & O'Connell 1993).

As for the occurrence of RR Lyrae pulsators, Figure 2 also shows that if log $Z \leq -5$ the ZAHB location of the models is, in all cases, hotter than the RR Lyrae instability strip, independently of the assumption on the cluster age. As a consequence, one cannot expect ZAHB pulsators nor is it possible to rely any further on the widely used HB parameter as given by the luminosity level of the ZAHB at log $T_e = 3.85$. Note that a moderate increase of the maximum stellar mass (i.e., a decrease of the cluster age) cannot help. In fact, the 1.0 $M_\odot$ ZAHB models are already near the minimum temperature that marks the turnover of metal-deficient ZAHBs toward larger temperatures. Only a further substantial decrease in age, removing the electron degeneracy from the He core of the evolving RGs and thus decreasing the value of $M_{cH\text{-}F}$, will be able to push newborn He-burning stars at lower effective temperatures toward the RG branch.

However, Figure 2 shows that the instability strip will be reached by the large majority of models during post-ZAHB evolution. To discuss this point in more detail, Figure 3 shows the evolution with time of effective temperature for all the models with masses equal to or larger than 0.55 $M_\odot$. Inspection of Figure 3 reveals that, fairly independently of the cluster age, for each given metallicity there is a minimum mass that experiences the RR Lyrae pulsational instability during the major phase of central He burning. According to the nonmonotonic dependence of $M_{cHe\text{-}F}$ on the metal content, one finds that this mass is on the order of 0.70 $M_\odot$ when log $Z = -5$, increasing to $\sim$0.75 $M_\odot$ for log $Z = -6$ and coming back toward 0.70 $M_\odot$ at log $Z = -10$.

Concerning the nonmonotonic behavior of $M_{cHe\text{-}F}$ versus metallicity, one finds that metal-deficient stars behave as normal metal-poor stars down to log $Z = -6$, with increasing $M_{cHe\text{-}F}$ when the metallicity is decreased. The decrease of $M_{cHe\text{-}F}$ when going further down to log $Z = -10$ is easily understood by remembering that in such low-mass stars, the temperature of the H-burning shell is so high that the H shell burning is powered by self-produced carbon (see Paper I). Since the thermal state of the core is determined by the heat inflow from the H shell burning, the core is much hotter at a given core mass, and the core mass at the He ignition is then smaller (see also Fujimoto et al. 1995).

As a result, depending on the previous evolutionary history and, in particular, on the amount of mass loss and

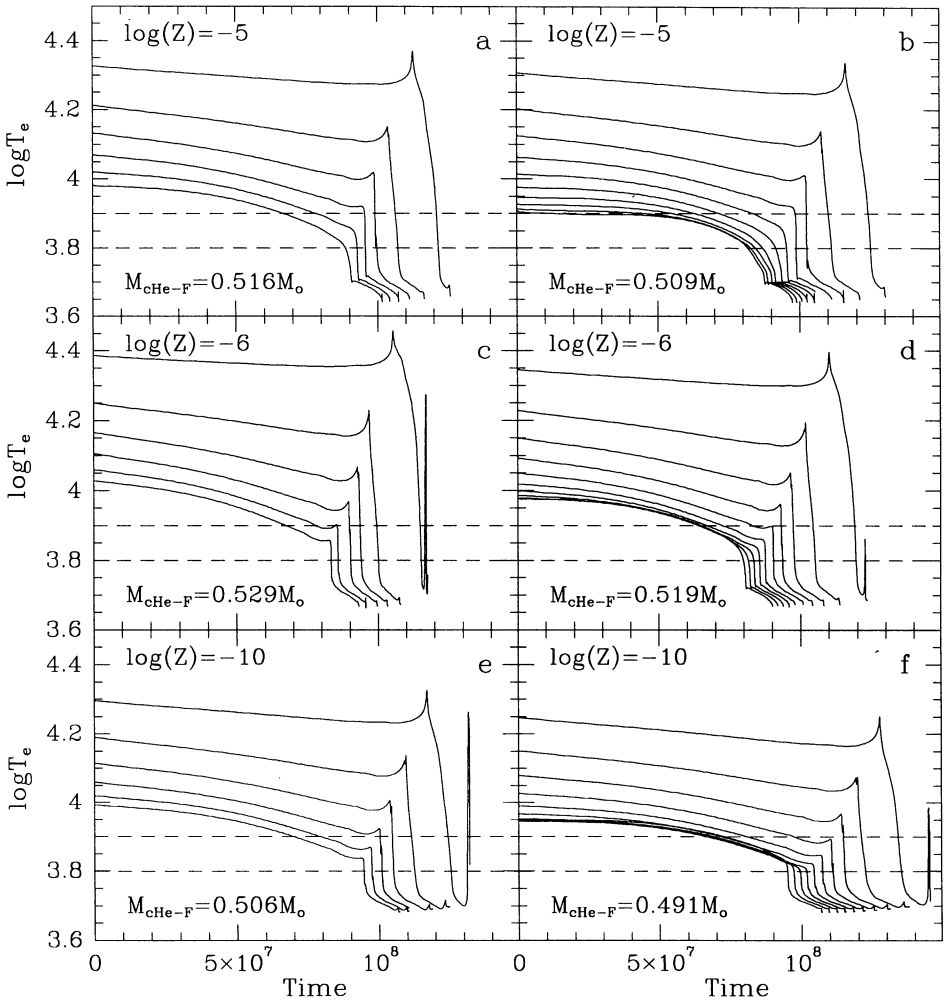

FIG. 3.—Behavior with time of the effective temperature of all the computed HB models for the labeled assumptions about the star's metallicity. Left and right panels, show, respectively, models with a 0.8 $M_\odot$ and 1.0 $M_\odot$ progenitor. Dashed lines show the approximate boundaries of the RR Lyrae instability strip.

on the cluster age, parameters that govern the maximum mass of the evolving stars, the occurrence of RR Lyrae stars cannot be excluded. In any instance, it can be predicted that the existence of RR Lyrae pulsators of the aforementioned metallicity should be a rather infrequent occurrence.

In fact, the data in Figure 3 show that when $\log Z = -6$ and for a cluster age of 15×10^9 yr (i.e., for an original mass of HB stars of 0.8 $M_\odot$), only those stars that would reach the HB phase with practically no mass loss should experience the RR Lyrae pulsational instability, an occurrence that—in addition—will last only ~20% of their central He–burning lifetimes. As a whole, we feel that there is a very small probability of finding similar pulsators, a chance that is only slightly increased by moving the metallicity in the explored range. Decreasing the cluster age, the probability of finding RR Lyrae pulsators increases slightly, essentially because of the increased amount of allowed mass loss.

One may finally note that as the edges of the instability strip do not depend on metallicity, no peculiar periods are expected for metal-deficient RR Lyrae stars, since both masses and luminosities of metal-deficient pulsators remain in the range experienced by more metal-rich RR Lyrae variables.

We end this section by noting that the existence of metal-deficient RR Lyrae pulsators may be challenged by an additional occurrence. In fact, Hollowell, Iben, & Fujimoto (1990) suggest that at the He core flash of a zero-metal star CNO nuclei are dredged up to the surface at a level that the ZAHB progenitor of a former zero-metal star would contain a CNO abundance on the order of $X_{CNO} \sim 0.004$ (but still devoid of iron). This occurrence will also affect, to some extent, a fraction of the metal-deficient stars, mostly those toward the lower end of the metallicity range. Of course the occurrence of such a dredge-up will modify the properties of the H-burning shell and, therefore, the location of the star on the H-R diagram in such a way as to shift the star models toward the red side of the ZAHB (Castellani & Tornambè 1977).

3. ADVANCED PHASES OF He BURNING

3.1. *The Early AGB Phase*

In this section we discuss the evolutionary phase that follows the central He exhaustion, from the onset of He burning in a shell up to the moment at which the luminosity provided by the He shell declines and the power supply comes to be provided by the H shell. The phase is generally referred to as early AGB (E-AGB).

In Figure 4 we show the temporal behavior of the surface luminosities all along the He-burning phases that precede

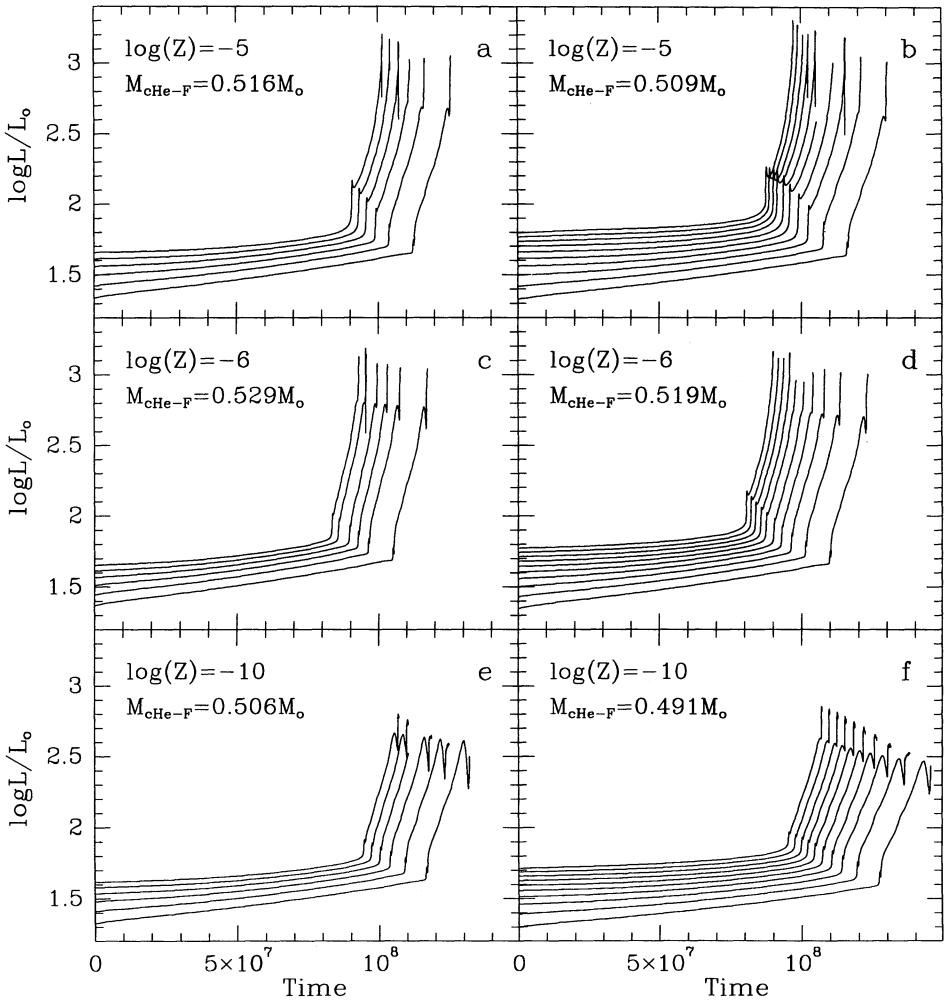

FIG. 4.—Behavior with time of the luminosity of all the He-burning models for the labeled values of metallicity and for a 0.8 $M_\odot$ (*left*) and 1.0 $M_\odot$ (*right*) progenitor.

the thermally pulsing AGB. In this figure, one can easily recognize the steady increase in luminosity, which corresponds to the phase of central He burning, followed by the sudden increase when the star leaves the HB to reach the E-AGB and by the first maximum in luminosity, which marks the ignition of the He-burning shell. After this phase, the luminosity continues to grow rapidly, following the ascent of the star along the E-AGB until a second maximum is achieved, which marks the end of the He shell burning phase and the reignition of the H shell.

As a general feature, one finds that, by decreasing the metallicity, the E-AGB phase starts closer to the HB, so that one expects that at $\log Z = -10$ the basis of the E-AGB should lie at only ~ 0.25 mag above the HB. An inspection of Figure 4 reveals that both the occurrence of a first maximum in the luminosity and the luminosity level at which the maximum occurs appear to be correlated with the stellar mass and/or metallicity. The larger the metallicity and the mass, the more pronounced becomes the signature of this feature and the larger is the luminosity at which it is located. It appears that such behavior is correlated with the efficiency level attained by the H-burning shell during the critical phase following the sudden exhaustion of central He in a convective core and before He burning becomes well-settled in a shell. This occurrence is clearly shown in Figure 5, where we plot the contribution to the luminosity of the various nuclear energy sources all along the He-burning phases of 1.0 $M_\odot$ models endowed with various metallicities.

For models with $\log Z = -5$, one finds that the H-burning shell remains active during the major phase of central He burning, making a substantial contribution to the energy release at the moment at which central He burning vanishes. By decreasing the metallicity, the contribution of CNO burning progressively disappears, and the end of central He burning is marked by a sudden transition to the "He shell only" regime. Note that the $\log Z = -10$ model never succeeds in igniting the CNO cycle all along central or shell He burning, in spite of the evidence that the giant progenitor was burning hydrogen via CNO in a shell (see Paper I).

It appears that the efficiency of H shell burning again plays a role in the second maximum, which marks the vanishing of the He-burning shell's power supply. In normal stars, when the He shell arrives in the vicinity of the H-rich zone, nuclear burning shifts quite smoothly from the He shell burning regime to the H shell one, powered by the CNO cycle at the bottom of the H-rich envelope. This is exactly what happens to the more metal-rich small-mass star models in our sample (see, e.g., Fig. 6*a* for the metallicity $\log Z = -6$). However, when going toward larger values of the masses, one finds that helium reignites progressively earlier, so that, in the case of 1.0 $M_\odot$, H burning fails to reach the control of the structure before the onset of the He flash (Fig. 6*b*). One can regard such an occurrence as evidence for the transition toward the quiet double shell burning regime expected in even larger masses (as discussed in § 3.2).

It is worth noting that, in this evolutionary phase, $\log Z = -10$ structures succeed for the first time after their RG phase in producing fresh carbon nuclei, burning hydrogen near the threshold for 3 α reactions. As a consequence, in these stars *p-p* burning is rapidly substituted by CNO burning as the main source of energy during this phase.

As a whole, one finds that the second maximum in the luminosity appears to be related to the occurrence of H-supported structures. The farther one moves toward lower metallicities and/or smaller masses, the more one is moving toward *hard-to-ignite* He-burning shells; as a consequence, H burning succeeds more and more in substituting He shell burning in the control of the structure.

In $\log Z = -10$ star models, the declining of He shell burning is followed by a rather dramatic series of events.

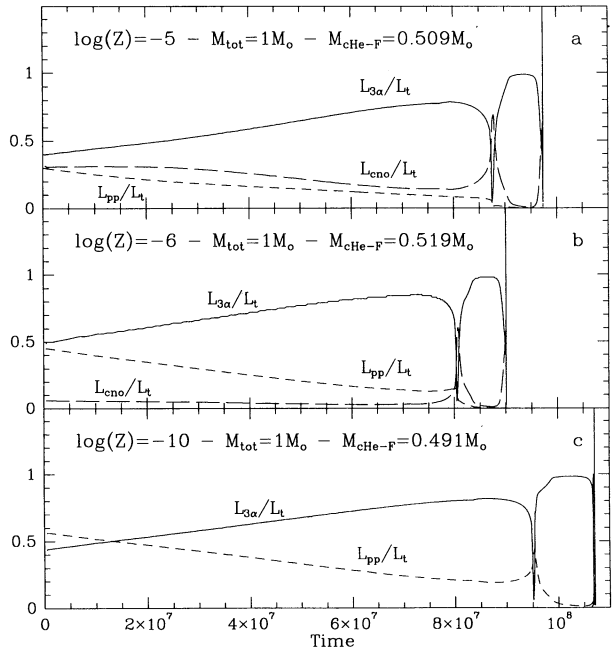

FIG. 5.—Behavior with time of the nuclear energy sources all along the He-burning phases for models of 1.0 $M_\odot$ and the labeled values of metallicity.

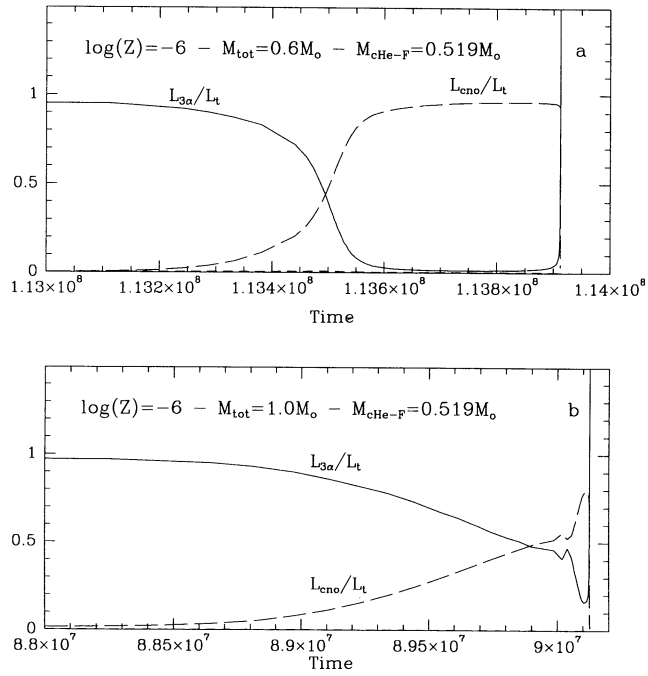

FIG. 6.—Behavior with time of nuclear energy sources at the reignition of the H shell for a model of 0.6 $M_\odot$ (*top*) and 1.0 $M_\odot$ (*bottom*) for the labeled value of metallicity.

Eventually *p-p* burning reignites with a microflash that heats the region until carbon is produced and CNO burning dominates the still-growing flash.

In the next section it will become clear how this scenario can be understood in terms of low power demand to the H-burning shell in stellar structures with low mass and low metallicity.

3.2. *The* He *Intershell Accretion Phase and onset of the First Thermal Pulse*

The occurrence of thermal pulses along the AGB phase was early recognized by Schwarzschild & Härm (1965). Extended investigations into the physical properties of stellar structures suffering thermal pulses have been successively performed by Iben (1975, 1976, 1977, 1982) in a series of papers and by others (for a detailed reference see Iben & Renzini 1983).

Later, it was found that thermal pulses were suppressed in a 5 $M_\odot$ zero-metal star (Chieffi & Tornambè 1984). In a companion paper (Fujimoto et al. 1984), it was also suggested that there exists a threshold, in core mass and CNO abundance, for the existence of thermal pulses.

Fujimoto et al. (1984) analyzed the properties of H and He shell burning in AGB stars by means of a generalized, semianalytical method developed by Fujimoto (1982), establishing that the time variation of a temperature perturbation δT can be written as

$$\frac{\partial \delta T}{\partial t} = \frac{\epsilon_r}{c_P T} F \delta T , \qquad (1)$$

where ϵ_r is the rate of heat diffusion, c_P is the specific heat at constant pressure, and F is a complicate function of various thermodynamic quantities (see eqs. [15]–[17] of Fujimoto et al. 1984). The stability criterion is connected to the value assumed by the parameter F. If at any point F is greater than zero, He shell burning is thermally unstable; when F is everywhere less than zero, He shell burning is stable.

According to such a criterion, they found that, in absence of CNO nuclei, the stability of He shell burning depends on the mass of the C-O core (M_{CO}) at the beginning of the AGB phase, which has to be compared with a critical core-mass value $M_{CO}^{crit} \approx 0.73\ M_\odot$. For $M_{CO} \leq M_{CO}^{crit}$, the criterion is violated, and recurrent shell flashes are expected to occur. If $M_{CO} > M_{CO}^{crit}$, He shell burning succeeds in settling into a steady state. M_{CO}^{crit} assumes a value that depends on the initial amounts of CNO nuclei. Increasing the initial abundance of CNO nuclei increases the value of M_{CO}^{crit}.

This theory agrees with the results of Chieffi & Tornambè (1984) since the core mass of their 5 $M_\odot$ zero-metal star model was 0.78 $M_\odot$, larger than $\sim 0.73\ M_\odot$, the limiting core mass to have thermal pulses when Z_{CNO} is zero.

For zero-metal structures these occurrences can be plainly understood as follows: In the case of rather massive cores, the energy demand to the H shell is such to require that hydrogen is burned at a very high temperature. As a consequence, 3 α reactions are at work in the H shell (where they produce carbon nuclei for the CNO cycle), and, a fortiori, they are fully active in the inner (hotter) He shell. The two shells proceed outward in mass at the same rate (Chieffi & Tornambè 1984). Thus the growth of the intershell mass and the development of thermal pulses is prevented. Conversely, in the case of less massive cores, the lower energy demand requires H shell burning temperatures that do not necessarily imply that 3 α reactions must be fully active in the He shell. All the cases analyzed in this paper, even those with an extremely low metal content, lie in the range of parameters for which Fujimoto et al. (1984) suggested that thermal instabilities occur because of the low core mass.

However, as a peculiar feature, it is now found that at the onset of the He shell flash an unusually huge amount of energy is produced. In order to analyze in detail the physical properties of these models, let us follow the evolution through the first He shell flash of the 0.8 $M_\odot$ star model with metallicity $\log Z = -10$ and He core mass on the ZAHB equal to 0.506 $M_\odot$. In the following, the evolutionary results of this model will be compared with those of a 0.8 $M_\odot$ star model with metallicity $\log Z = -3$ and He core mass on the ZAHB equal to 0.494 $M_\odot$, computed for comparison and referred to as "normal."

The value assumed by the parameter F in the $\log Z = -10$ model is ~ 4.7—as obtained by means of an interpolation between data shown in Table 1 of Fujimoto et al. (1984). This value is significantly lower than expected for a star with a similar core mass with solar metallicity (~ 14.3), but large enough to *push* the structure in the range of parameters for which a thermally unstable configuration is expected to occur.

In fact, as it happens in "normal" structures, as soon as H shell burning resumes, the He-burning shell switches off and the intershell mass starts again to grow. During this phase the H shell temperature settles at around $\log T \approx 7.98$, a value not far from $\log T_1 \approx 8.02$ predicted by Fujimoto et al. (1984), as derived by means of an extrapolation from their Figure 6.

However, two main structural differences with respect to "normal" models are already noticeable at this point. The first is that the minimum intershell mass attained by the very low metallicity model is remarkably smaller than what is usually attained in "normal" models. The second difference is that the H-burning shell accretes the intershell mass at a rate smaller than is found in the "normal" case. Both occurrences are easy to explain. The first is due to the fact that a larger temperature is required to ignite a very metal poor H shell (thus the He-burning shell must move closer to the H-rich zone). The second difference arises from the fact that in a very metal poor H-burning shell hydrogen is converted into helium with a rather low efficiency.

Once reignited, the H shell induces (as expected) structural changes that determine a substantial switching off of the He-burning shell (as occurs also in "normal" models). The burning level at which the He shell settles (i.e., the temperature and density levels) depends also on the rate at which the overlying H shell is accreting by mass the intershell zone. In fact, the thermal behavior of this zone is determined by the timescale at which energy is locally deposited by the gravitational settling of freshly synthesized helium nuclei (and by the timescale at which energy is transferred to the remaining structure, a quantity that should always remain shorter than, or comparable with, the nuclear timescale). Both the decrease of the He shell temperature and the increase of its density are of amounts markedly larger than in a "normal" model. It is worth noting that in the very metal poor experiment, the He shell attains temperature and density values for which a mild electron degeneracy develops ($\psi \approx 2$), in contrast with the "normal" models, in which this shell does not become degenerate (in our comparison model, $\psi \approx -1$).

Moreover, because of the reduced efficiency of the H shell, the amount of fresh matter that must be added to the intershell layer in order to induce the He shell reignition is larger than in the "normal" case. It has to be noted, however, that the reignition occurs in both cases when the intershell mass is $\sim 0.038\ M_\odot$, with the difference that in the "normal" case the intershell mass runs between 0.034 and 0.039 $M_\odot$, while in the very metal poor model it runs between 0.027 and 0.038 $M_\odot$. Accordingly, the intershell accreting timescale changes.

Because of the mild degeneracy level at which the He shell of the very low metal model has settled during the H-accretion phase, the strength of the He pulse occurring in these models is markedly stronger than it is in "normal" models. As soon as sufficient He-rich matter has been accreted to the intershell layer, a very powerful He flash develops. As a consequence, a convective shell develops, rapidly growing in size. Quite soon, convection reaches the H-rich layers and penetrates inside them, adding fresh protons to the very hot zones in which the He flash is developing. The consequence is that the release of nuclear energy is suddenly even more enhanced and so is the extension of the convective layer. From this point on, our code was unable to follow in detail the further evolution since a time-dependent mixing should be taken into account.

The upper panel of Figure 7 shows the temporal behavior of the hydrogen and helium luminosities during the He intershell accretion phase of the $\log Z = -10$ star model up to the onset of the He shell flash. The lower panel illustrates the same quantities but for the model with initial metallicity $\log Z = -3$ computed for comparison and previously defined as "normal." Both panels cover the same time interval, a choice that allows one to appreciate the different timescales on which the pulse develops in the two structures. While for $\log Z = -10$ our calculations end at the moment of hydrogen injection into the He shell for the reasons discussed earlier, for the model with $\log Z = -3$ we also see the first pulse and interpulse phase. At the point at which the data of the upper panel end, the 3 α energy release is still far from the point of its maximum power but already more than 2 orders of magnitudes larger than the maximum attained during the pulse of the "normal" structure.

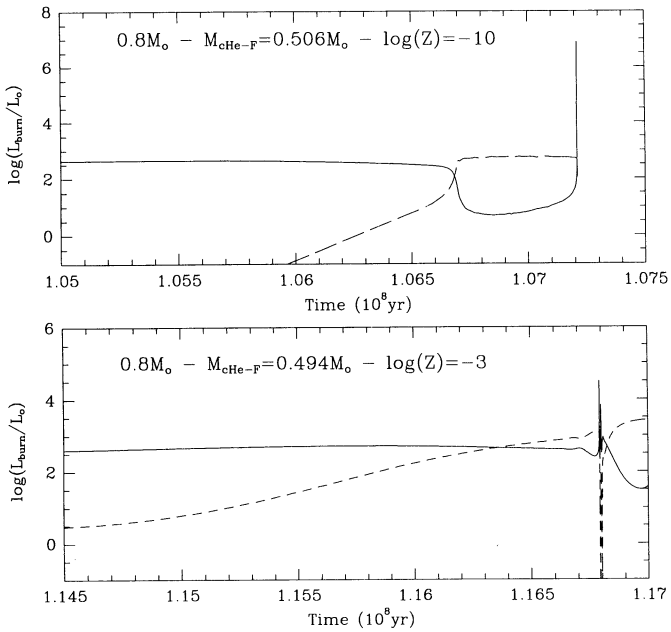

FIG. 7.—Temporal behavior of the hydrogen (*dashed lines*) and helium (*solid lines*) luminosities during the first episode of He intershell accretion phase in the $Z = 10^{-10}$ star model (*top*) and in a model with initial metallicity $Z = 10^{-3}$ defined as "normal" in § 3.2. Data for the model with $Z = 10^{-10}$ end at the moment of hydrogen injection into the He shell, where computations are halted. Even if the flash is here much more powerful than the flash in the "normal" structure, it is still far from the point of its maximum energy release. Note that in both panels the covered time interval is 2.5×10^6 yr.

In fact, by not allowing protons to be mixed into the He layer, we obtain an estimate of the maximum energy that can be delivered during the pulse by He burning alone. With this trick it has been possible to entirely follow the flash up to the point of maximum energy release and beyond. At its maximum, the He-burning luminosity turned out to be $2.5 \times 10^8\ L_\odot$ as opposed to a maximum release of $7.5 \times 10^4\ L_\odot$ during the first pulse of the "normal" model. At its maximum extent, convection would have entered the H envelope by $\Delta M \sim 0.005\ M_\odot$, a quantity that would imply a hydrogen amount of $M_H \sim 2.4 \times 10^{30}$ g to be injected into a $\Delta M \sim 0.04\ M_\odot$ thick convective shell to be burned at temperatures larger than 2.3×10^8 K.

It is reasonable, however, to expect that in the real world protons injected into the He shell are burned during their flight to the bottom of the He shell, with consequences on the evolution that are not easy to evaluate and about which we will nevertheless speculate in the next section.

4. DISCUSSION AND CONCLUSIONS

To explore the further evolutionary behavior of the models discussed above is not an easy task since it is at least necessary to employ a time-dependent convection, a procedure not yet developed at a trustworthy level. Nevertheless, let us speculate on the possible outcomes so as to learn, from these models, a lesson that may be relevant in a similar (even if not equivalent) evolutionary occurrence, as in the off-center detonation of an He layer in an H-accreting white dwarf.

First of all, we can figure out the outcome if the mixing timescales are longer than the H-burning timescale. In this occurrence, hydrogen is convected down to the bottom of the He-burning convective shell and burned there at high temperature. It is possible to estimate the amount of energy released in such an occurrence and the relative timescale. In a few seconds, some 10^{48} ergs will be stored at the bottom of the H envelope. Such a power release is able to determine an overpressure comparable to that required to expel the envelope.

However, with a slightly more realistic approach, one can estimate the mixing timescale by means of the mixing-length theory. Coupling these data with the local burning timescales inside the He-burning convective shell, one obtains the result that fresh protons will not arrive at the bottom of the He-burning shell but will be burned right at halfway, on a timescale of a few hundred seconds. In fact, across the inner half of the convective shell, the temperature and density changes are not so steep to determine several orders of magnitude changes of the burning timescale. Once again, to a first approximation, one would conclude that the energy-release timescales and the amount of released energy would be such as to make it difficult to avoid a dynamical outcome.

However, studying the He core flash of a low-mass, $Z = 0$ stellar model, Hollowell et al. (1990) encountered a very

similar occurrence. In their model, the He flash at the end of the RG phase occurred so off-center that the H envelope was soon involved in the convective layer formed upon He ignition.

Using an algorithm to treat time-dependent convection, they obtained the result that, at a given moment, H burning becomes so strong as to release more energy than He burning. As a consequence, two convective shells formed, one linked with He burning, the other with the H-burning front, the outcome being a peculiar, but not dynamical, He core flash. A similar result had previously been obtained by Sweigart (1974) by forcing protons to be mixed into the convective shell during a He shell flash if the ingestion rate grows over a given value.

The same occurrence may happen in the present models. In such a case, when the strength of the He pulse decreases, because of the decreased amount of fuel, the same will happen in the H shell. H burning is likely to resume soon in a slightly more external shell, and a very unusual series of thermal pulses may follow. As a matter of fact, even if the further evolution of the model previously discussed can at present only be conjectured, there remains strong evidence that a large amount of hydrogen surrounding the He shell is consumed upon the development of an unusually strong He flash.

One can attempt to translate such an occurrence into a much more general scenario. The occurrence of a strong He flash, that in our single star is a consequence of the low metallicity, is expected as the result of moderate accretion ($10^{-9}\ M_\odot\ \mathrm{yr}^{-1} \leq \dot{M} \leq 10^{-8}\ M_\odot\ \mathrm{yr}^{-1}$) of the He layers by a companion star in a binary system (Limongi & Tornambè 1991). Thus the explored behavior can shed light on the case in which the He shell flash takes place in a layer located at the top of a matter-accreting white dwarf and involves an He shell massive enough that a supernova event is the outcome, i.e., a flash much stronger than the one occurring in the stellar structure studied in this work, and dynamical in itself. The outcome will be a supernova in which a peculiar central C detonation is triggered by the explosion occurring in the outer He layer (Woosley & Weaver 1994). It may occur that most, if not all, Type Ia supernovae may be produced by such a mechanism. If so, and if the accretion occurs from a normal H-rich companion (Munari & Renzini 1992), there would still remain the problem of the absence of hydrogen lines in the observed spectra of Type Ia supernovae. (This is not the only problem in such a model; in fact, the accretion of the He layer through an H-burning shell requires a very finely tuned accretion rate.) The evidence discussed in this paper, that the occurrence of a strong He shell flash induces a stronger flash in the surrounding H layer, may represent the natural explanation for the absence of hydrogen in Type Ia supernovae, at least when these originate from a sub-Chandrasekhar mass model. In fact, the amount of hydrogen burned out and the timescale on which the combustion would take place should be respectively large and short enough to make it conceivable that most of the surrounding hydrogen is burned out in the event that precedes by ~ 1 s the full explosion of the dwarf. (Since to obtain a sub-Chandrasekhar He detonation the required H-accretion rates should range between $\dot{M} \sim 5 \times 10^{-9}\ M_\odot\ \mathrm{yr}^{-1}$ and $\dot{M} \sim 5 \times 10^{-8}\ M_\odot\ \mathrm{yr}^{-1}$, an H atmosphere of at most $1\ M_\odot$ can be expected.) In addition, the possibility must be considered that a peculiar nucleosynthesis occurs in the region where hydrogen is burned at an unusually high temperature.

REFERENCES

Bono, G., Castellani, V., Degl'Innocenti, S., & Pulone, L. 1995, A&A, 297, 115
Cassisi, S., & Castellani, V. 1993, ApJS, 88, 509 (Paper I)
Castellani, V., Chieffi, A., & Pulone, L. 1991, ApJS, 76, 911
Castellani, V., Chieffi, A., & Straniero, O. 1992, ApJS, 78, 517
Castellani, V., & Tornambè, A. 1977, A&A, 61, 427
Chieffi, A., & Tornambè, A. 1984, ApJ, 287, 745
Dorman, B., Rood, R. T., & O'Connell, R. W. 1993, ApJ, 419, 596
Fujimoto, M. Y. 1982, ApJ, 257, 767
Fujimoto, M. Y., Iben, I., Jr., Chieffi, A., & Tornambè, A. 1984, ApJ, 287, 749
Fujimoto, M. Y., Sugiyama, K., Iben, I., Jr., & Hollowell, D. 1995, ApJ, 444, 175
Hollowell, D., Iben, I., Jr., & Fujimoto, M. Y. 1990, ApJ, 351, 245
Iben, I., Jr. 1975, ApJ, 196, 525
———. 1976, ApJ, 208, 165
Iben, I., Jr. 1977, ApJ, 217, 788
———. 1982, ApJ, 260, 821
Iben, I., Jr., & Renzini, A. 1983, ARA&A, 21, 271
Limongi, M., & Tornambè, A. 1991, ApJ, 371, 317
Molaro, P., & Bonifacio, P. 1990, A&A, 236, L5
Molaro, P., & Castellani, F. 1990, A&A, 228, 426
Munari, U., & Renzini, A. 1992, ApJ, 397, L87
Norris, J. E., Peterson, R. C., & Beers, T. C. 1993, ApJ, 415, 797
Primas, F., Molaro, P., & Castelli, F. 1994, A&A, 290, 885
Sandage, A. 1990, ApJ, 350, 603
Schwarzschild, M., & Härm, R. 1965, ApJ, 142, 855
Sneden, C., Preston, G. W., McWilliam, A., & Searle, L. 1994, ApJ, 431, L27
Sweigart, A. V. 1974, ApJ, 189, 289
Woosley, S. E., & Weaver, T. A. 1994, ApJ, 423, 371